



Published in final edited form as:

Histochem Cell Biol. 2011 May ; 135(5): 475–485. doi:10.1007/s00418-011-0806-2.

Expression and roles of Slit/Robo in human ovarian cancer

Cai Feng Dai,

Department of Obstetrics and Gynecology, Qilu Hospital of Shandong University, Jinan 250012, Shandong, People's Republic of China

Department of Obstetrics and Gynecology, University of Wisconsin, PAB1 Meriter Hospital, 202 S. Park St, Madison, WI 53715, USA

Yi Zhou Jiang,

Department of Obstetrics and Gynecology, University of Wisconsin, PAB1 Meriter Hospital, 202 S. Park St, Madison, WI 53715, USA

Yan Li,

Department of Obstetrics and Gynecology, University of Wisconsin, PAB1 Meriter Hospital, 202 S. Park St, Madison, WI 53715, USA

Kai Wang,

Department of Obstetrics and Gynecology, University of Wisconsin, PAB1 Meriter Hospital, 202 S. Park St, Madison, WI 53715, USA

Pei Shu Liu,

Department of Obstetrics and Gynecology, Qilu Hospital of Shandong University, Jinan 250012, Shandong, People's Republic of China

Manish S. Patankar, and

Department of Obstetrics and Gynecology, University of Wisconsin, PAB1 Meriter Hospital, 202 S. Park St, Madison, WI 53715, USA

Jing Zheng

Department of Obstetrics and Gynecology, University of Wisconsin, PAB1 Meriter Hospital, 202 S. Park St, Madison, WI 53715, USA

Jing Zheng: jzheng@wisc.edu

Abstract

The Slit glycoproteins and their Roundabout (Robo) receptors regulate migration and growth of many types of cells including human cancer cells. However, little is known about the expression and roles of Slit/Robo in human ovarian cancer. Herein, we examined the expression of Slit/Robo in human normal and malignant ovarian tissues and its potential participation in regulating migration and proliferation of human ovarian cancer cells using two ovarian cancer cell lines, OVCAR-3 and SKOV-3. We demonstrated that Slit2/3 and Robo1 were immunolocalized primarily in stromal cells in human normal ovaries and in cancer cells in many histotypes of ovarian cancer tissues. Protein expression of Slit2/3 and Robo1/4 was also identified in OVCAR-3 and SKOV-3 cells. However, recombinant human Slit2 did not significantly affect SKOV-3 cell

© Springer-Verlag 2011

Correspondence to: Jing Zheng, jzheng@wisc.edu.

Present Address:

K. Wang, Central Laboratory, Shanghai First Maternity and Infant Hospital, Tongji University School of Medicine, Shanghai 200040, People's Republic of China

Conflict of interest The authors have declared that no competing interests exist.

migration, and OVCAR-3 and SKOV-3 cell proliferation. Slit2 also did not induce ERK1/2 and AKT1 phosphorylation in OVCAR-3 and SKOV-3 cells. The current findings indicate that three major members (Slit2/3 and Robo1) of Slit/Robo family are widely expressed in the human normal and malignant ovarian tissues and in OVCAR-3 and SKOV-3 cells. However, Slit/Robo signaling may not play an important role in regulating human ovarian cancer cell proliferation and migration.

Keywords

Slit; Robo; Ovarian cancer; ERK1/2; AKT; Migration; Proliferation

Introduction

Although there have been great advances in our understanding of ovarian cancer biology and significant improvement in surgical technology and therapy regimens over the last three decades, the mobility and mortality of ovarian cancer remain high with an estimated 21,880 new cases and 13,850 deaths in the USA alone in 2010 (American Cancer Society at <http://www.cancer.org> 2010). This high mortality is largely due to the fact that the majority (~70%) of ovarian cancer is diagnosed at an advanced, chemoresistant stage (Wang et al. 2010). To date, the cellular and molecular pathogenesis of human ovarian cancers is poorly understood (Bast et al. 2009), even though it is believed that approximately 90% of primary malignant ovarian tumors arise from the ovarian surface epithelium (Bell 2005). Therefore, a better understanding of the cellular and molecular pathogenesis of ovarian cancer will assist the development of novel therapeutic interventions for this deadly gynecological disease.

The secreted Slit glycoproteins and their Roundabout (Robo) receptors, consisting of three Slit (Slit1–3) and four Robo (Robo1–4) members in vertebrates, were originally identified in the nervous system as a repulsive cue to prevent axons from migrating to inappropriate locations during the assembly of the nervous system (Andrews et al. 2007; Brose et al. 1999). Each mammalian Slit contains four leucine-rich regions (Robo-binding domains), nine epidermal growth factor repeats, a laminin G domain, and a C-terminal cysteine-rich domain (Hohenester 2008). Slits can be proteolytically cleaved into the N- and C-terminal fragments *in vivo* and *in vitro* (Ba-Charvet et al. 2001; Brose et al. 1999; Little et al. 2001; Patel et al. 2001). It is believed that only full length and the N-terminus, both of which are predominantly membrane bound, of the Slits can bind and activate Robos (Ba-Charvet et al. 2001; Brose et al. 1999; Little et al. 2001; Patel et al. 2001). Robos belong to the Ig superfamily of transmembrane signaling molecules (Hohenester 2008; Morlot et al. 2007). Robo1–3 consist of five Ig-like and three type III fibronectin domains in the ectodomain, whereas Robo4 has only two Ig domains. To date, the specific high-affinity Slit binding has been demonstrated biochemically for all Robos, except for Robo4 (Hohenester 2008; Morlot et al. 2007).

As many Slit/Robo family members are detected in a variety of non-nervous tissues, critical roles of the Slit/Robo signal in regulating growth, development, and remodeling of these non-nervous tissues have been recognized (Dickinson and Duncan 2010; Hinck 2004; Ypsilanti et al. 2010). This notion is firmly supported by the observation that homozygous knockout of Slit1/2/3 (Liu et al. 2003; Plump et al. 2002; Yuan et al. 2003) and Robo1/2 (Grieshammer et al. 2004; Xian et al. 2001) often results in impaired development of lungs, hearts, and kidneys, leading to newborn death shortly after birth.

Recently, Slit/Robo has also been identified in major organs of the female reproductive system including fetal and adult ovaries, endometria, and placentas (Dickinson et al. 2008; Dickinson and Duncan 2010; Dickinson et al. 2010; Duncan et al. 2010; Ma et al. 2010). In sheep fetal ovary, Slit/Robo is present primarily in oocytes of the primordial follicles, and its increased expression is accompanied by a reduction in the number of proliferating oocytes in the developing ovary (Dickinson et al. 2010). The Slit/Robo family members have also been detected in luteal cells and stromal cells of the human adult ovary, in which blockade of Slit/Robo activity promotes cell migration and decreases apoptosis in primary cultured luteal cells, suggesting that Slit/Robo may regulate lute-olysis in women (Dickinson et al. 2008).

Slit/Robo is expressed in many types of human cancers (Legg et al. 2008; Liao et al. 2010b). Nonetheless, reports on the roles of Slit/Robo in human cancers are controversial. It has been postulated that Slit/Robo may function as a tumor suppressor (Legg et al. 2008; Liao et al. 2010b; Narayan et al. 2006). This is supported by several lines of evidence. First, homozygous deletion of *ROBO1* gene is detected in lung and breast carcinomas (Sundaresan et al. 1998). Second, Slit2 is able to suppress the growth of breast and colorectal tumor cells (Dallol et al. 2002a, b, 2003), and the Slit/Robo signal is often inactivated in breast, lung, colorectal, and brain cancers by hypermethylation of the Slit and Robo promoters (Dallol et al. 2002a, b, 2003; Dickinson et al. 2004; Morris et al. 2003). Third, the expression of certain Slit/Robo members is decreased in many cancer tissues, including lung cancer, breast cancer, adult renal cell carcinoma, cervical cancer, and prostate cancer (Dallol et al. 2002a, b; Latil et al. 2003; Ma et al. 2010; Tanno et al. 2006), as compared to normal tissues or less advanced cancer tissues. In contrast, increased expression of certain Slit/Robo members has also been reported in prostate cancer (Latil et al. 2003), breast cancer (Tanno et al. 2006), colorectal cancer (Grone et al. 2006), hepatocellular carcinoma (Ito et al. 2006), lung, kidney, liver, and metastatic melanoma (Seth et al. 2005). Furthermore, a recent report has shown that neutralization of Robo1 reduces the cancer mass and the microvascular density of human malignant melanoma in vivo, suggesting that Slit/Robo may promote cancer growth and development, plausibly via promoting cancer angiogenesis (Wang et al. 2003). Thus, Slit/Robo might either promote or inhibit cancer development, depending on individual type of cancers.

Little is known about the expression and roles of Slit/Robo in human ovarian cancer. Herein, we examined the expression of Slit2/3 and Robo1/4, four major members of Slit/Robo in human normal and malignant ovary tissues, as well as SKOV-3 and OVCAR-3 cells, two human ovarian cancer cell lines. We also examined the potential participation of the Slit/Robo signal in regulating migration and proliferation of SKOV-3 and OVCAR-3 cells.

Materials and methods

Human ovarian tissue microarray and human ovarian cancer cell lines

Human ovarian cancer tissue microarrays (cat # OV2084) were purchased from Biomax, Rockville, MD, USA. This tissue microarray contains 16 normal ovarian tissue samples (NORM; including eight adjacent normal ovarian and eight normal ovarian tissues) and 192 cases of ovarian cancer. Cancer histotypes include adult granular cell tumor (AGCT; $n = 4$), disgerminoma (DISG; $n = 5$), adenocarcinoma (ADEN; $n = 8$), teratoma malignant change (TMC; $n = 5$), yolk sac tumor (YST; $n = 6$), mucinous adenocarcinoma (Mu-ADEN; $n = 20$), serous adenocarcinoma (Se-ADEN; $n = 136$, in which 21 were classified as low grade (L-Se-ADEN) and 115 as high grade (H-Se-ADEN) based on the 2-tie grading system) (Ayhan et al. 2009; Malpica et al. 2004).

Human ovarian adenocarcinoma cell lines, OVCAR-3 and SKOV-3, were obtained from the American Type Culture Collection (Manassas, VA, USA). OVCAR-3 cells were expanded

in RPMI1640 medium (Invitrogen, Carlsbad, CA, USA) containing 10% FBS (HyClone, Logan, UT, USA), 1% penicillin/streptomycin (HyClone), and 10 µg/ml insulin (Sigma, St. Louis, MO, USA). SKOV-3 cells were expanded in RPMI 1640 medium containing 10% FBS and 1% penicillin/streptomycin. Each cell line was maintained in a humidified atmosphere containing 5% CO₂ at 37°C.

Immunohistochemistry

Immunolocalization of Slit2/3 and Robo1/4 in the human ovarian cancer tissue microarray was carried out as described (Jiang et al. 2010; Zheng et al. 1999). Immunoreactivity of Slit2/3 and Robo1/4 was visualized by indirect detection with the avidin–biotin complex kit (Vector Laboratories, Burlingame, CA, USA) using 3-amino-9-ethylcarbazole (Vector Laboratories) as a chromogen. After deparaffinization, the tissue microarray underwent antigen retrieval in a 10-mM citrate buffer solution (pH 6.0) in a microwave. Endogenous peroxidase activity was quenched in 0.3% H₂O₂. The tissue microarray was lightly counterstained with hematoxylin (Fisher Scientific, Pittsburg, PA, USA). After blocking the nonspecific binding with 1% horse serum albumin, the tissue microarray was probed with a goat antibody against an internal region of human Slit2 (cat # sc-16619), the C-terminus of human Slit3 (cat # sc-31597) (4 µg/ml; Santa Cruz Biotechnology, Santa Cruz, CA, USA) or a rabbit antibody against human Robo1 (cat # ab7279), or Robo4 (cat # ab10547) (4 µg/ml; Abcam, Cambridge, MA, USA). After washing, the tissue microarray was incubated with a biotinylated secondary antibody. Two more tissue microarrays were probed with preimmune goat and rabbit IgG, respectively, at 4 µg/ml as negative controls. The staining was examined and recorded under a Nikon microscope equipped with a Spot Insight QE CCD camera.

Staining intensity of Slit2/3 and Robo1/4 was semi-quantitatively analyzed as described (Jiang et al. 2010). The images from the cancer tissues with the sample size per cancer histotype ≥ 4 were taken under a 10 \times objective, which represented $\sim 83\%$ of area of each tissue core. The images were uniformly converted to 8-bit grayscale pictures. The integrated optical density (OD) value was measured by the MetaMorph analysis software (Molecular Devices, Sunnyvale, CA, USA). All data reported were corrected by subtracting the OD value of the IgG control in each corresponding section. Since no significant difference in Slit2/3 and Robo1/4 staining intensity was observed between adjacent normal ovarian tissues and normal ovarian tissues, data from these two types of tissues were pooled.

Western blot analysis for Slit2/3, Robo1/4, ERK1/2, and AKT1

To determine the expression of Slit2/3 and Robo1/4 in OVCAR-3 and SKOV-3 cells, Western blot analysis was performed as described (Jiang et al. 2010; Wang et al. 2008; Zheng et al. 1999). OVCAR-3 and SKOV-3 cells were cultured as above. Cells were lysed by sonication in buffer [50 mM HEPES, 0.1 M NaCl, 10 mM EDTA, 4 mM sodium pyrophosphate, 10 mM sodium fluoride, 2 mM sodium orthovanadate (pH 7.5), 1 mM PMSF, 1% Triton X-100, 5 µg/ml leupeptin, 5 µg/ml aprotinin]. After centrifugation, protein concentrations of the supernatant were determined with BSA (fraction V; Sigma, St. Louis, MO, USA) as standards. The protein samples (50 µg) were separated on 8% or 4–15% gradient SDS-PAGE gels and electrically transferred to PVDF membranes. Human hepatoblastoma cell lysate (50 µg, cat # sc2227; Santa Cruz Biotechnology) and mouse thyroid extract (50 µg, cat # sc2407; Santa Cruz Biotechnology) were run in parallel as positive controls for Slit2 and Slit3, respectively, as recommended by the manufacturer. Human umbilical cord vein endothelial (HUVE) cells were used as the positive control for Robo1/4 (Wang et al. 2003). The membranes were probed with a rabbit antibody against the C-terminus of human Slit2 (1: 200; cat # sc-28945), the N-terminus of human Slit3 (1: 200; cat # sc-28946; Santa Cruz Biotechnology), or Robo1 (1:1,000; cat # Ab7279) or Robo4

(1:1,000; cat # Ab10547; Abcam), followed by reprobing with a mouse GAPDH (1:20,000; cat # H00002597-M01; Abnova, Walnut, CA) or β -actin (1:4,000; Ambion, Austin, TX, USA) as a loading control. Proteins were visualized using enhanced chemiluminescence reagents (Amersham Biosciences, Piscataway, NJ, USA), followed by exposure to chemiluminescence films. The immunoreactive signals were analyzed by a densitometer. HUVE cells were isolated from term placentas of normal pregnant women. Collection of placentas was approved by the Institutional Review Board, Meriter Hospital, and the Health Sciences Institutional Review Boards, the University of Wisconsin- Madison, and followed the recommended guidelines for using human subjects.

To determine if Slit2 activates ERK1/2 and AKT1, additional OVCAR-3 and SKOV-3 cells were cultured as above. After serum starvation for 16 h, cells were treated without or with 100 ng/ml of recombinant human Slit2 protein (Cat # ab82131, Abcam) for 0, 10, 30 min, 1 h, and 3 h. The protein (15 μ g) was subjected to Western blotting as described (Wang et al. 2008; Zheng et al. 1999). For each set of samples, at least two gels were run simultaneously. One membrane was blotted with a phospho-ERK1/2 antibody, followed by reblotting with a total ERK1/2 antibody (both were at 1:2,000). Another membrane was blotted with a phospho-AKT1 antibody (1:500) followed by reblotting with a total AKT1 antibody (1:2,000). All of these four antibodies were purchased from Cell Signaling Technology, Beverly, MA, USA. The membranes were also reprobbed with a mouse GAPDH (1:10,000; cat # H00002597-M01; Abnova, Walnut, CA, USA). Proteins were visualized using chemiluminescence reagents (Amersham, Piscataway, NJ, USA). Changes in total and phospho-ERK1/2 and AKT1 protein levels were quantified by a densitometer. Data on phospho-ERK1/2 and AKT1 were normalized to total ERK1/2 and AKT1. Data on total ERK1/2 and AKT1 were normalized to GAPDH.

Cell migration

Cell migration was evaluated using a 24-Multiwell BD Falcon FluoroBlok Insert System (8.0 μ m pores; BD Biosciences, San Jose, CA, USA) as described (Liao et al. 2010a). After serum starvation for 24 h, 30,000 cells were seeded in the insert (topside of membrane) and cultured in serum-free media. Slit2 (final concentration 100 ng/ml) in media containing 0.5% heat-inactivated FBS or media containing 0.5% heat-inactivated FBS as a control was added into the bottom wells. After 16 h, cells that migrated to the bottom of the inserts were stained with calcein AM (0.2 μ g/ml; Invitrogen) for 30 min, examined, and recorded by an inverted microscope mounted with a CCD camera. The numbers of migrated cells were counted using the MetaMorph image analysis software (Molecular Devices). HUVE cells were run in parallel in a similar fashion as a positive control (Wang et al. 2003).

Cell proliferation

Cell proliferation assay was carried out as described (Wang et al. 2008; Zheng et al. 1999). Cells seeded in 96-well plates (5,000 cells/well) were cultured in complete growth media. After 16 h of serum starvation, cells were treated with Slit2 at 0, 5, 10, or 100 ng/ml (6 wells/dose). Media without or with Slit2 (100 ng/ml) were changed every 2 days. After 4 days of culture, the number of cells was determined using the crystal violet method. Briefly, cells were rinsed with distilled water and air dried. Once dried, cells were lysed with 2% (w/v) sodium deoxycholate solution with gentle agitation. Absorbance was measured at 570 nm on a microplate reader (BioTek Instrument, Winooski, VT, USA). Wells containing known cell numbers (0, 1,000, 2,000, 5,000, 10,000, 20,000, or 40,000 cells/well; 6 wells/cell density) were used to establish standard curves.

Wound healing assay

To confirm Slit2's action on ovarian cancer cell migration and proliferation, the wound healing assay was performed as described (Liao et al. 2010a). OVCAR-3 and SKOV-3 cells were cultured on 12-well plates in complete growth media, until reaching confluence, and serum starved overnight. A sterilized 200- μ l pipette tip was used to make a straight scratch, simulating a wound. Cells were washed once with serum-free media and then treated without or with recombinant human Slit2 (100 ng/ml; cat # ab82131, Abcam) in serum-free media up to 24 h. Five images per scratch, which represented 60% of the length of each scratch, were photographed under a 4 \times objective immediately after scratching, and after 16 and 24 h of Slit treatment. Sizes of the wound area (mm^2) were calculated using the MetaMorph image analysis software (Molecular Devices).

Statistics procedures

Data for the Slit/Robo staining intensity in the tissue microarrays and changes in ERK1/2 and AKT1 phosphorylation in OVCAR-3 and SKOV-3 cells were analyzed using one-way ANOVA followed by pairwise comparisons (SigmaStat; Jandel Co., San Rafael, CA, USA). Data for the Slit/Robo protein levels in human ovarian cancer cells were analyzed using the Student's *t* test. $p \geq 0.05$ was considered to be significant.

Results

Immunolocalization of Slit/Robo in human ovarian cancer tissues

Positive staining for Slit2/3 and Robo1, but not Robo4 was present in NORM, primarily in stromal cells (Fig. 1A–D). The immunoreactivity of Slit2/3 and Robo1/4 was also found in cancer cells in several histotypes of ovarian cancer tissues (Fig. 1A–D). In Mu-ADEN and Se-ADEN, Slit2/3 and Robo1/4 were localized primarily in epithelial cells (Fig. 1A–D). No staining was observed in the preimmune goat or rabbit IgG control (see the small inserts in h panels of Fig. 1A–D). The semi-quantitative analysis revealed that for each target protein examined, there was no significant difference in staining intensity between the grades, stages, and TNM classifications in each histotype of ovarian cancer, except Se-ADEN (Fig. 1E).

For Slit2 (Fig. 1A), immunoreactivity was present in AGCT, primarily in granulosa cells, DISG, and YST, as well as in ADEN, Mu-ADEN, L-Se-ADEN, and H-Se-ADEN, primarily in epithelial cells. The overall staining intensity was relatively high in NORM, AGCT, DISG, YST, Mu-ADNE, L-Se-ADEN, and H-Se-ADEN as compared to that in ADEN and TMC. A semi-quantitative analysis confirmed these observations. However, due to high variation of staining intensity and relatively small sample sizes in certain histotypes of ovarian cancers, significant ($p \geq 0.05$) differences in the staining intensity were detected only in YST and L-Se-ADEN as compared to NORM (Fig. 1E).

For Slit3 (Fig. 1B), the strong staining was seen in DISG and YST, while weak staining was presented in NORM, ADEN, AGCT, Mu-ADEN, TMC, L-Se-ADEN, and H-Se-ADEN. The semi-quantitative analysis also indicated that the staining was much more ($p \geq 0.05$) intensive in DISG and YST than in the others (Fig. 1E). These differences in the staining intensity were in agreement with data from the semi-quantitative analysis (Fig. 1E).

For Robo1 (Fig. 1C), moderate and strong staining was observed in NORM and all histotypes of ovarian cancer. The semi-quantification analysis revealed that the staining intensity in DISG, YST, Mu-ADEN, L-Se-ADEN, and H-Se-ADEN was significantly higher ($p \geq 0.05$) than that in NORM, AGCT, ADEN, and TMC (Fig. 1E).

For Robo4 (Fig. 1D), the overall staining was weak in NORM and all histotypes of ovarian cancer tissues except DISG, in which the staining was more intensive than that in all other tissues. These observations were confirmed by the semi-quantitative analysis (Fig. 1E).

Expression of Slit2/3 and Robo1/4 in OVCAR-3 and SKOV-3 cells

The antibody against the C-terminus of human Slit2 detected a band at ~50 kDa in OVCAR-3, SKOV-3, and human hepatoblastoma cells (the positive controls) (Fig. 2). The molecular mass of 50 kDa corresponds to the C-terminus of human Slit2 reported (Ba-Charvet et al. 2001; Brose et al. 1999; Little et al. 2001; Patel et al. 2001). No band was detected at ~200 kDa (the full length Slit2) and ~140 kDa (the N-terminus of Slit2) (Ba-Charvet et al. 2001; Brose et al. 1999; Patel et al. 2001). The Slit2 antibody also detected an additional band right below 50 kDa in SKOV-3 cells (Fig. 2). It is currently unknown if this band represents a unique isoform or a truncated form of Slit2 in SKOV-3 cells.

The antibody against the N-terminus of human Slit3 detected two strong bands at ~65 and 45 kDa, as well as a weak band at ~100 kDa in OVCAR-3 and SKOV-3 cells, and also in the positive control (mouse thyroid extract) (Fig. 2). These ~65 and 45 kDa bands might represent the C-terminus of Slit3 as previously reported for Slit3 (Little et al. 2001) and Slit1/2 (Ba-Charvet et al. 2001; Brose et al. 1999; Little et al. 2001; Patel et al. 2001). No band was detected for Slit3 at ~200 kDa (the full-length Slit3; data not shown) and ~140 kDa (the N-terminus of Slit3; data not shown) (Ba-Charvet et al. 2001; Little et al. 2001; Patel et al. 2001). The Robo1/4 antibodies detected a single band at ~250 and 170 kDa, respectively, in OVCAR-3, SKOV-3, and HUVE cells (the positive control) (Fig. 2). Both of these molecular masses correspond to human Robo1/4 reported (Seki et al. 2010; Wang et al. 2003). These data indicate the expression of Slit2/3 and Robo1/4 in OVCAR-3 and SKOV-3 cells.

Activation of ERK1/2 and AKT1

As compared to the control, recombinant human Slit2 at 100 ng/ml did not significantly induce ERK1/2 and AKT1 phosphorylation up to 3 h (Fig. 3). It, however, is noted that the basal level (time 0) of total ERK1/2, but not phospho ERK1/2 in SKOV-3 cells, was much higher ($p \geq 0.05$) than that in OVCAR-3 cells; however, the basal level of phospho AKT1 but not total AKT1 in SKOV-3 was higher than that in OVCAR-3 cells (Table 1).

Effects of Slit2 on cell migration, proliferation, and wound healing

Under a serum-free condition, SKOV-3 underwent migration (Fig. 4). However, no cell migration was observed for OVCAR-3 cells under a similar serum-free condition and even after 10% FBS stimulation (data not shown). Slit2 at 100 ng/ml promoted ($p \geq 0.05$) HUVE cell migration by 27% over the control in agreement with the previous report (Wang et al. 2003). Treatment of Slit2 did not alter SKOV-3 (Fig. 4) and OVCAR-3 (data not shown) cell migration.

After 4 days of treatment, the number of SKOV-3 cells ($10,703 \pm 556.9$) in the control was increased approximately by twofold of the initially seeding cells, while no significant change was observed for OVCAR-3 cells ($4,585 \pm 574.1$). As compared to the control, Slit2 slightly increased (~112% of the control) the number of OVCAR-3 cells at 5, 10, and 100 ng/ml, but this stimulatory effect did not reach significance (Fig. 5). Treatment of Slit2 also did not affect SKOV-3 cell numbers (Fig. 5).

Treatment of Slit2 did not affect wound healing in both OVCAR-3 and SKOV-3 cells (Fig. 6). In OVCAR-3 cells, the scratch areas did not show significant changes either in the control or in Slit2 treatment up to 24 h. In SKOV-3 cells, the scratch areas were similar

between the control and Slit treatment at 16 h, whereas these were almost healed and not detectable in both the control and Slit2 treatment at 24 h (Fig. 6). These data confirm that Slit2 has no effect on proliferation and migration of SKOV-3 cells as described in Figs. 4 and 5.

Discussion

In the current study, we have demonstrated, for the first time as far as we are aware, the protein expression of three members (Slit2/3 and Robo1) of Slit/Robo family in the adult human normal ovary tissue and in a variety of histotypes of human ovarian cancer tissues, suggesting that Slit/Robo might play an important role in both normal and malignant ovarian tissues. However, given that Slit2 did not affect cell proliferation and migration of ovarian cancer cells, the role of the Slit/Robo signaling in regulating human ovarian cancer cell function remains to be identified.

Among four Slit/Robo family members studied, Slit2/3 and Robo1 were relatively widely present in human normal and malignant ovarian tissues, while Robo4 was localized only in a few histotypes of ovarian cancer tissues (i.e., DISG, YST, and H-Se-ADEN). These data suggest that Slit proteins could function as autocrine or paracrine factors in human ovarian normal and malignant cancer. Moreover, as compared to Robo4, higher levels of Robo1 in normal ovarian tissues and many histotypes of ovarian cancer tissues studied also imply that Robo1 is a major receptor for Slit in both normal and malignant ovarian tissues. This is in agreement with previous reports showing that Robo1 is the major receptor for Slit proteins in the non-nervous system (Mertsch et al. 2008). It is noteworthy that for each Slit/Robo family member, expression levels were highly varied across different histotypes of ovarian cancer, albeit it could be partially attributed to the small sample size in some of these histotypes of cancer. This highly uneven expression of Slit/Robo is not surprising since human ovarian cancer is characterized by its high heterogeneity (Bast et al. 2009). Moreover, our observations that Robo1 levels in DISG, YST, and Se-ADEN were ~2.5 to 3.7-fold higher than those in NORM imply that Robo1 could serve as a diagnostic marker for these major histotypes of human ovarian cancer and/or could potentially be used as a therapeutic target for these ovarian cancers after its role is defined.

It is believed that Robo4 is exclusively expressed in endothelial cells, particularly in tumors (Neri and Bicknell 2005), and mediates Slit2-inhibited VEGF₁₆₅-induced in vitro angiogenesis and VEGF₁₆₅-induced in vivo vascular permeability (Jones et al. 2008). In contrast, blockade of Robo using a Robo neutralizing antibody could suppress the growth of human malignant melanoma cells in vivo, possibly via inhibiting tumor angiogenesis (Wang et al. 2003). Nonetheless, in the current study, regardless of whether Slit/Robo was pro- or anti-angiogenic, no apparent immunoreactivity of Robo4, and also Robo1 was detected in vascular endothelial cells in normal and malignant ovarian tissues. Thus, it is unlikely that Slit2 can directly target endothelial cells via binding to Robo1/4 in these ovarian tissues to affect ovarian angiogenesis.

The downstream signaling of Slit remains largely unknown. However, previous reports have implied that Slit2 could function via activating the MEK/ERK1/2 and PI3K/AKT1 signaling pathways in human malignant melanoma (Wang et al. 2003) and Xenopus retinal growth cones (Piper et al. 2006). Our current observations that Slit2 did not alter ERK1/2 and/or AKT1 phosphorylation in OVCAR-3 and SKOV-3 cells up to 3 h suggest that both ERK1/2 and AKT1, two key signaling molecules in mediating many essential cell processes (Kolch 2000), do not directly participate in mediating Slit2's actions in both of these cancer cell lines. It is noteworthy that the basal level of total ERK1/2 and phospho AKT1 in SKOV-3 cells was much higher than that in OVCAR-3 cells. It is currently unclear if such differential

regulation has impacts on different behaviors (e.g., different growth rates) between these two cell lines.

In the current study, we detected mainly the C-terminus, but not full length and N-terminus of Slit2/3 in OVCAR-3 and SKOV-3 cells. These data suggest that the proteolytic fragments (Hohenester 2008) are the major forms of Slit2/3 existing in human ovarian cancer cells as in other non-tumor tissues (Hohenester 2008), and the majority of the N-terminus of Slit2/3 is rapidly released out and dissociate from ovarian cancer cells after their cleavage from the full length of Slit2/3. Given that the C-terminus of Slit2 is biologically inactive (Ba-Charvet et al. 2001; Patel et al. 2001), these C-terminal fragments of Slit2/3 should not play an important role in regulating ovarian cancer cell function. In contrast, the N-terminal fragments of Slit2/3 after their releases from the cells might act on ovarian cancer cells.

In recent years, most members of the Slit/Robo family have been found in many solid tumors, but their roles in the progression of various cancers have not been clearly defined. The association of high Robo1 levels with DISG, YST, and Se-ADEN supports the notion that the Slit/Robo is pro-cancer in human ovarian cancer, as suggested in many other cancers including endometrial cancer (Narayan et al. 2006), prostate cancer (Latil et al. 2003), breast cancer (Tanno et al. 2006), colorectal cancer (Grone et al. 2006), hepatocellular carcinoma (Ito et al. 2006), lung, kidney, liver, and metastatic melanoma (Seth et al. 2005), and malignant melanoma (Wang et al. 2003). However, in the current in vitro study, we observed that Slit2 did not affect cell proliferation and migration in both OVCAR-3 and SKOV-3 cells, although it stimulated migration of HUVE cells. Thus, we speculate that Slit/Robo may participate in regulating other ovarian cancer functions such as cell differentiation and apoptosis (Chédotal et al. 2005). For example, Slit2 might regulate cell apoptosis in human ovarian cancer, particularly since SKOV-3 and OVCAR-3 cells either keep proliferating (SKOV-3) or maintain their cell number (OVCAR-3) at the initial plating level even after 4 days of serum starvation as observed in the current study.

Acknowledgments

This work was supported in part by the National Institutes of Health grants HL64703 and HD38843 (JZ).

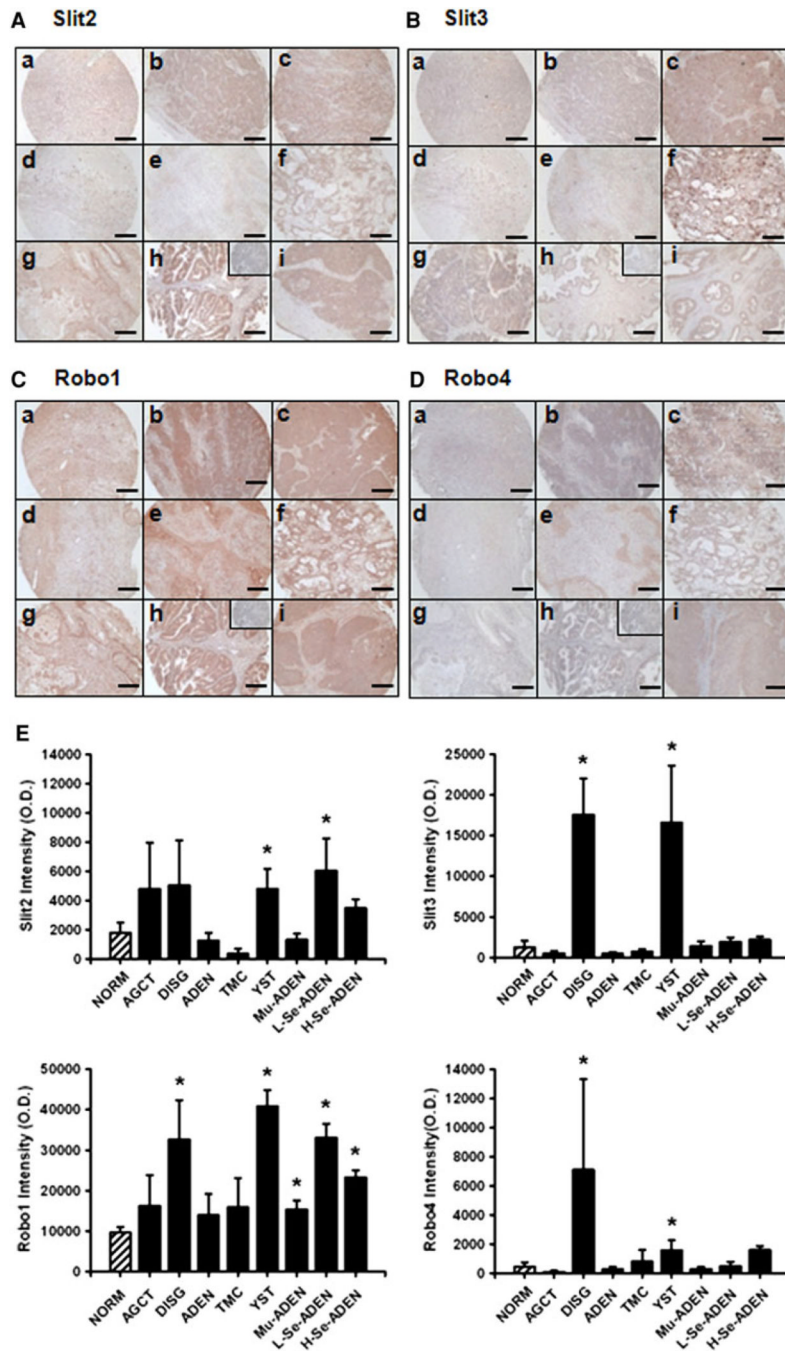
References

- American Cancer Society at <http://www.cancer.org>: Cancer Facts & Figures. 2010.
- Andrews WD, Barber M, Parnavelas JG. Slit–Robo interactions during cortical development. *J Anat.* 2007; 211:188–198. [PubMed: 17553100]
- Ayhan A, Kurman RJ, Yemelyanova A, Vang R, Logani S, Seidman JD, Shihle M. Defining the cut point between low-grade and high-grade ovarian serous carcinomas: a clinicopathologic and molecular genetic analysis. *Am J Surg Pathol.* 2009; 33:1220–1224. [PubMed: 19461510]
- Ba-Charvet KTN, Brose K, Ma L, Wang KH, Marillat V, Sotelo C, Tessier-Lavigne M, Chédotal A. Diversity and specificity of actions of Slit2 proteolytic fragments in axon guidance. *J Neurosci.* 2001; 21:4281–4289. [PubMed: 11404413]
- Bast RC, Hennessy B, Mills GB. The biology of ovarian cancer: new opportunities for translation. *Nat Rev Cancer.* 2009; 9:415–428. [PubMed: 19461667]
- Bell DA. Origins and molecular pathology of ovarian cancer. *Mod Pathol.* 2005; 18 Suppl 2:S19–S32. [PubMed: 15761464]
- Brose K, Bland KS, Wang KH, Arnott D, Henzel W, Goodman CS, Tessier-Lavigne M, Kidd T. Slit proteins bind Robo receptors and have an evolutionarily conserved role in repulsive axon guidance. *Cell.* 1999; 96:795–806. [PubMed: 10102268]
- Chédotal A, Kerjan G, Moreau-Fauvarque C. The brain within the tumor: new roles for axon guidance molecules in cancers. *Cell Death Differ.* 2005; 12:1044–1056. [PubMed: 16015381]

- Dallol A, Da Silva NF, Viacava P, Minna JD, Bieche I, Maher ER, Latif F. SLIT2, a human homologue of the Drosophila Slit2 gene, has tumor suppressor activity and is frequently inactivated in lung and breast cancers. *Cancer Res.* 2002a; 62:5874–5880. [PubMed: 12384551]
- Dallol A, Forgacs E, Martinez A, Sekido Y, Walker R, Kishida T, Rabbitts P, Masher ER, Minna JD, Latif F. Tumour specific promoter region methylation of the human homologue of the Drosophila Roundabout gene DUTT1 (ROBO1) in human cancers. *Oncogene.* 2002b; 21:3020–3028. [PubMed: 12082532]
- Dallol A, Morton D, Masher ER, Latif F. SLIT2 axon guidance molecule is frequently inactivated in colorectal cancer and suppresses growth of colorectal carcinoma cells. *Cancer Res.* 2003; 63:1054–1058. [PubMed: 12615722]
- Dickinson RE, Duncan WC. The SLIT–ROBO pathway: a regulator of cell functions with implications for the reproductive system. *Reproduction.* 2010; 139:697–704. [PubMed: 20100881]
- Dickinson RE, Dallol A, Bieche I, Krex D, Morton D, Maher ER, Latif F. Epigenetic inactivation of SLIT3 and SLIT1 genes in human cancers. *Br J Cancer.* 2004; 91:2071–2078. [PubMed: 15534609]
- Dickinson RE, Myers M, Duncan WC. Novel regulated expression of the SLIT/ROBO pathway in the ovary: possible role during luteolysis in women. *Endocrinology.* 2008; 149:5024–5034. [PubMed: 18566128]
- Dickinson RE, Hryhorskyj L, Tremewan H, Hogg K, Thomson AA, McNeilly AS, Duncan WC. Involvement of the SLIT/ROBO pathway in follicle development in the fetal ovary. *Reproduction.* 2010; 139:395–407. [PubMed: 19900988]
- Duncan WC, McDonald SE, Dickinson RE, Shaw JLV, Lourenco PC, Wheelhouse N, Lee KF, Critchley HO, Horne AW. Expression of the repulsive SLIT/ROBO pathway in the human endometrium and fallopian tube. *Mol Hum Reprod.* 2010; 16:950–959. [PubMed: 20651036]
- Grieshammer U, Le M, Plump AS, Wang F, Tessier-Lavigne M, Martin GR. SLIT2-mediated ROBO2 signaling restricts kidney induction to a single site. *Dev cell.* 2004; 6:709–717. [PubMed: 15130495]
- Grone J, Doeblner O, Loddenkemper C, Hotz B, Buhr HJ, Bhargava S. Robo1/Robo4: differential expression of angiogenic markers in colorectal cancer. *Oncol Rep.* 2006; 15:1437–1443. [PubMed: 16685377]
- Hinck L. The versatile roles of ‘axon guidance’ cues in tissue morphogenesis. *Dev Cell.* 2004; 7:783–793. [PubMed: 15572123]
- Hohenester E. Structural insight into Slit–Robo signalling. *Biochem Soc Trans.* 2008; 36:251–256. [PubMed: 18363568]
- Ito H, Funahashi S, Yamauchi N, Shibahara J, Midorikawa Y, Kawai S, Kinoshita Y, Watanabe A, Hippo Y, Ohtomo T, Iwanari H, Nakajima A, Makuuchi M, Fukayama M, Hirata Y, Hamakubo T, Kodama T, Tsuchiya M, Aburatani H. Identification of ROBO1 as a novel hepatocellular carcinoma antigen and a potential therapeutic and diagnostic target. *Clin Cancer Res.* 2006; 12:3257–3264. [PubMed: 16740745]
- Jiang YZ, Wang K, Fang R, Zheng J. Expression of aryl hydrocarbon receptor in human placentas and fetal tissues. *J Histochem Cytochem.* 2010; 58:679–685. [PubMed: 20354149]
- Jones CA, London NR, Chen H, Park KW, Sauvaget D, Stockton RA, Wythe JD, Suh W, Larrieu-Lahargue F, Mukoyama YS, Lindblom P, Seth P, Frias A, Nishiya N, Ginsberg MH, Gerhardt H, Zhang K, Li DY. Robo4 stabilizes the vascular network by inhibiting pathologic angiogenesis and endothelial hyperpermeability. *Nat Med.* 2008; 14:448–453. [PubMed: 18345009]
- Kolch W. Meaningful relationships: the regulation of the Ras/Raf/MEK/ERK pathway by protein interactions. *Biochem J.* 2000; 351:289–305. [PubMed: 11023813]
- Latil A, Chene L, Cochant-Priollet B, Mangin P, Fournier G, Berthon P, Cussenot O. Quantification of expression of netrins, slits and their receptors in human prostate tumors. *Int J Cancer.* 2003; 103:306–315. [PubMed: 12471613]
- Legg JA, Herbert JM, Clissold P, Bicknell R. Slits and roundabouts in cancer, tumour angiogenesis and endothelial cell migration. *Angiogenesis.* 2008; 11:13–21. [PubMed: 18264786]

- Liao WX, Feng L, Zheng J, Chen DB. Deciphering mechanisms controlling placental artery endothelial cell migration stimulated by vascular endothelial growth factor. *Endocrinology*. 2010a; 151:3432–3444. [PubMed: 20463056]
- Liao WX, Wing DA, Geng JG, Chen DB. Perspectives of SLIT/ROBO signaling in placental angiogenesis. *Histol Histopathol*. 2010b; 25:1181–1190. [PubMed: 20607660]
- Little MH, Wilkinson L, Brown DL, Piper M, Yamada T, Stow JL. Dual trafficking of Slit3 to mitochondria and cell surface demonstrates novel localization for Slit protein. *Am J Physiol Cell Physiol*. 2001; 281:C486–C495. [PubMed: 11443047]
- Liu J, Zhang L, Wang D, Shen H, Jiang M, Mei P, Hayden PS, Sedor JR, Hu H. Congenital diaphragmatic hernia, kidney agenesis and cardiac defects associated with Slit3-deficiency in mice. *Mech Dev*. 2003; 120:1059–1070. [PubMed: 14550534]
- Ma S, Liu X, Geng JG, Guo SW. Increased SLIT immunoreactivity as a biomarker for recurrence in endometrial carcinoma. *Am J Obstet Gynecol*. 2010; 202:68.e1–68.e11. [PubMed: 19800604]
- Malpica A, Deavers MT, Lu K, Bodurka DC, Atkinson EN, Gershenson DM, Silva EG. Grading ovarian serous carcinoma using a two-tier system. *Am J Surg Pathol*. 2004; 28:496–504. [PubMed: 15087669]
- Mertsch S, Schmitz N, Jeibmann A, Geng JG, Paulus W, Senner V. Slit2 involvement in glioma cell migration is mediated by Robo1 receptor. *J Neurooncol*. 2008; 87:1–7. [PubMed: 17968499]
- Morlot C, Thielens NM, Ravelli RB, Hemrika W, Romijn RA, Gros P, Cusack S, McCarthy AA. Structural insights into the Slit–Robo complex. *Proc Natl Acad Sci USA*. 2007; 104:14923–14928. [PubMed: 17848514]
- Morris MR, Hesson LB, Wagner KJ, Morgan NV, Astuti D, Lees RD, Cooper WN, Lee J, Gentle D, Macdonald F, Kishida T, Grundy R, Yao M, Latif F, Maher ER. Multigene methylation analysis of Wilms' tumour and adult renal cell carcinoma. *Oncogene*. 2003; 22:6794–6801. [PubMed: 14555992]
- Narayan G, Goparaju C, Arias-Pulido H, Kaufmann AM, Schneider A, Dürst M, Mansukhani M, Pothuri B, Murty VV. Promoter hypermethylation-mediated inactivation of multiple Slit–Robo pathway genes in cervical cancer progression. *Mol Cancer*. 2006; 5:16. [PubMed: 16700909]
- Neri D, Bicknell R. Tumour vascular targeting. *Nat Rev Cancer*. 2005; 5:436–446. [PubMed: 15928674]
- Patel K, Nash JA, Itoh A, Liu Z, Sundaresan V, Pini A. Slit proteins are not dominant chemorepellents for olfactory tract and spinal motor axons. *Development*. 2001; 128:5031–5037. [PubMed: 11748139]
- Piper M, Anderson R, Dwivedy A, Weinl C, van Horck F, Leung KM, Cogill E, Holt C. Signaling mechanisms underlying Slit2-induced collapse of *Xenopus* retinal growth cones. *Neuron*. 2006; 49:215–228. [PubMed: 16423696]
- Plump AS, Erskine L, Sabatier C, Brose K, Epstein CJ, Goodman CS, Mason CA, Tessier-Lavigne M. Slit1 and Slit2 cooperate to prevent premature midline crossing of retinal axons in the mouse visual system. *Neuron*. 2002; 33:219–232. [PubMed: 11804570]
- Seki M, Watanabe A, Enomoto S, Kawamura T, Ito H, Kodama T, Hamakubo T, Aburatani H. Human ROBO1 is cleaved by metalloproteinases and gamma-secretase and migrates to the nucleus in cancer cells. *FEBS Lett*. 2010; 584:2909–2915. [PubMed: 20471383]
- Seth P, Lin Y, Hanai J, Shivalingappa V, Duyao MP, Sukhatme VP. Magic roundabout, a tumor endothelial marker: expression and signaling. *Biochem Biophys Res Commun*. 2005; 332:533–541. [PubMed: 15894287]
- Sundaresan V, Chung G, Heppell-Parton A, Xiong J, Grundy C, Roberts I, James L, Cahn A, Bench A, Douglas J, Minna J, Sekido Y, Lerman M, Latif F, Bergh J, Li H, Lowe N, Ogilvie D, Rabbitts P. Homozygous deletions at 3p12 in breast and lung cancer. *Oncogene*. 1998; 17:1723–1729. [PubMed: 9796701]
- Tanno T, Tanaka Y, Sugiura T, Akiyoshi H, Takenaka S, Kuwamura M, Yamate J, Ohashi F, Kubo K, Tsuyama S. Expression patterns of the slit subfamily mRNA in canine malignant mammary tumors. *J Vet Med Sci*. 2006; 68:1173–1177. [PubMed: 17146174]

- Wang B, Xiao Y, Ding BB, Zhang N, Yuan X, Gui L, Qian KX, Duan S, Chen Z, Rao Y, Geng JG. Induction of tumor angiogenesis by Slit–Robo signaling and inhibition of cancer growth by blocking Robo activity. *Cancer Cell*. 2003; 4:19–29. [PubMed: 12892710]
- Wang K, Song Y, Chen DB, Zheng J. Protein phosphatase 3 differentially modulates vascular endothelial growth factor and fibroblast growth factor 2-stimulated cell proliferation and signaling in ovine fetoplacental artery endothelial cells. *Biol Reprod*. 2008; 79:704–710. [PubMed: 18509162]
- Wang Y, Chan DW, Liu VW, Chiu P, Ngan HY. Differential functions of growth factor receptor-bound protein 7 (GRB7) and its variant GRB7v in ovarian carcinogenesis. *Clin Cancer Res*. 2010; 16:2529–2539. [PubMed: 20388850]
- Xian J, Clark KJ, Fordham R, Pannell R, Rabbitts TH, Rabbitts PH. Inadequate lung development and bronchial hyperplasia in mice with a targeted deletion in the Dutt1/Robo1 gene. *Proc Natl Acad Sci USA*. 2001; 98:15062–15066. [PubMed: 11734623]
- Ypsilanti AR, Zagar Y, Chedotal A. Moving away from the midline: new developments for Slit and Robo. *Development*. 2010; 137:1939–1952. [PubMed: 20501589]
- Yuan W, Rao Y, Babiuk RP, Greer JJ, Wu JY, Ornitz DM. A genetic model for a central (septum transversum) congenital diaphragmatic hernia in mice lacking Slit3. *Proc Natl Acad Sci USA*. 2003; 100:5217–5222. [PubMed: 12702769]
- Zheng J, Bird IM, Melsaether AN, Magness RR. Activation of the mitogen-activated protein kinase cascade is necessary but not sufficient for basic fibroblast growth factor- and epidermal growth factor-stimulated expression of endothelial nitric oxide synthase in ovine fetoplacental artery endothelial cells. *Endocrinology*. 1999; 140:1399–1407. [PubMed: 10067868]

**Fig. 1.**

Immunohistochemical analysis of Slit2/3 and Robo1/4 in human ovarian cancer tissue microarray. Immunolocalization of Slit2 (**A**), Slit3 (**B**), Robo1 (**C**), and Robo4 (**D**) was performed as described in “Materials and Methods”. *Reddish color* indicates positive Slit and Robo staining. For each target protein, representative images from NORM (*a*), AGCT (*b*), DISG (*c*), ADEN (*d*), TMC (*e*), YST (*f*), Mu-ADEN (*g*), L-Se-ADEN (*h*), and H-Se-ADEN (*i*) are shown. For the goat (**A**, **B**) or rabbit (**C**, **D**) preimmune IgG control, representative images from the L-Se-ADEN are shown. *Bar* 200 μ m. For the semiquantitative analysis of the Slit/Robo staining intensity (**E**), data are expressed as means \pm SEM of the integrated OD. *Differs from NORM ($p \leq 0.05$)

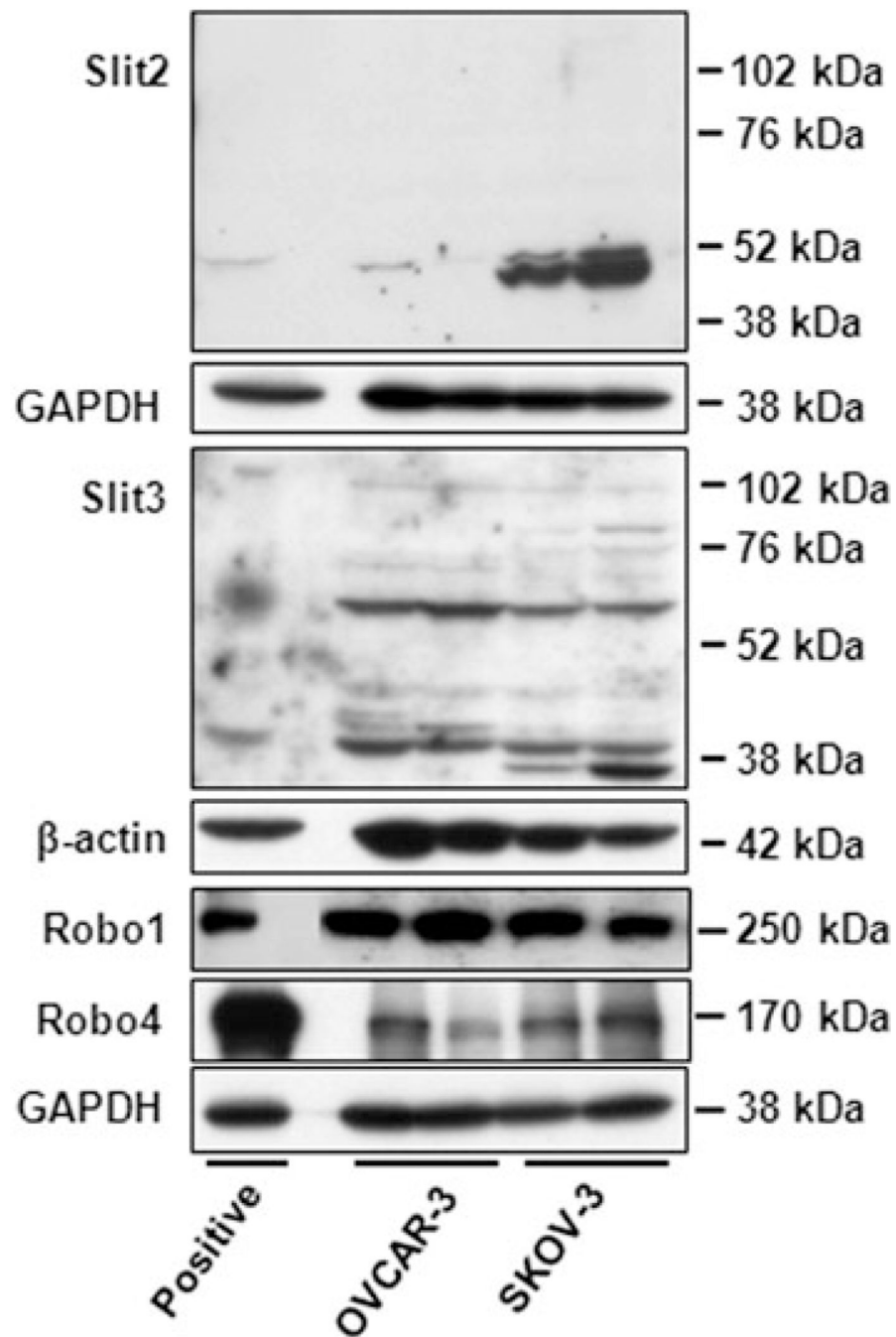


Fig. 2. Western blot analysis for Slit2/3 and Robo1/4 in OVCAR-3 and SKOV-3 cells. Cells at 80–90% confluence were harvested and subjected to Western blotting for Slit2/3 and Robo1/4. Different lanes in each individual ovarian cancer cell line represent different passages of cells. Positive controls for Slit2, Slit3, and Robo1/4 are human hepatoblastoma cell lysate, mouse thyroid extract, and HUVE cells, respectively

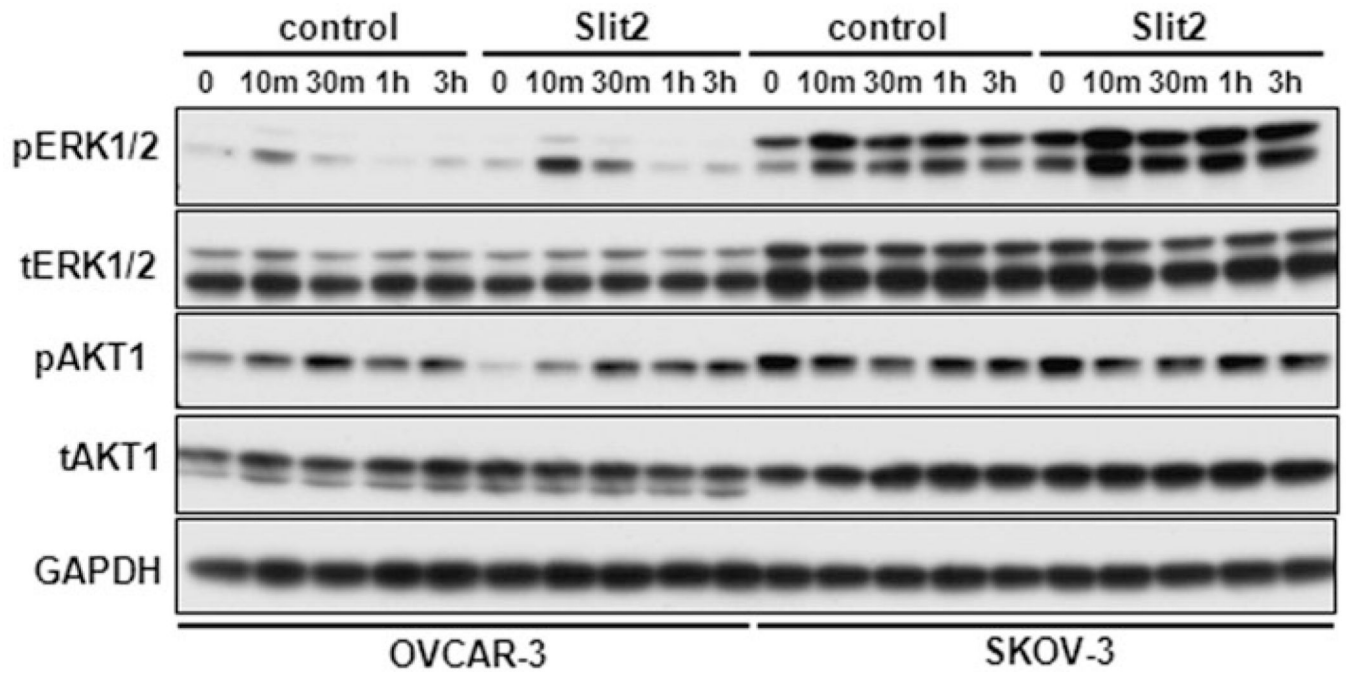


Fig. 3. Effects of Slit2 on phosphorylation of ERK1/2 and AKT1 in OVCAR-3 and SKOV-3 cells. After serum starvation for 16 h, cells at 80–90% confluence were treated with Slit2 (100 ng/ml) up to 3 h. Proteins were subjected to Western blotting for total (*t*) or phospho (*p*) ERK1/2 and AKT1. A representative Western blot from four independent experiments was shown for each target protein. *m* minutes, *h* hours

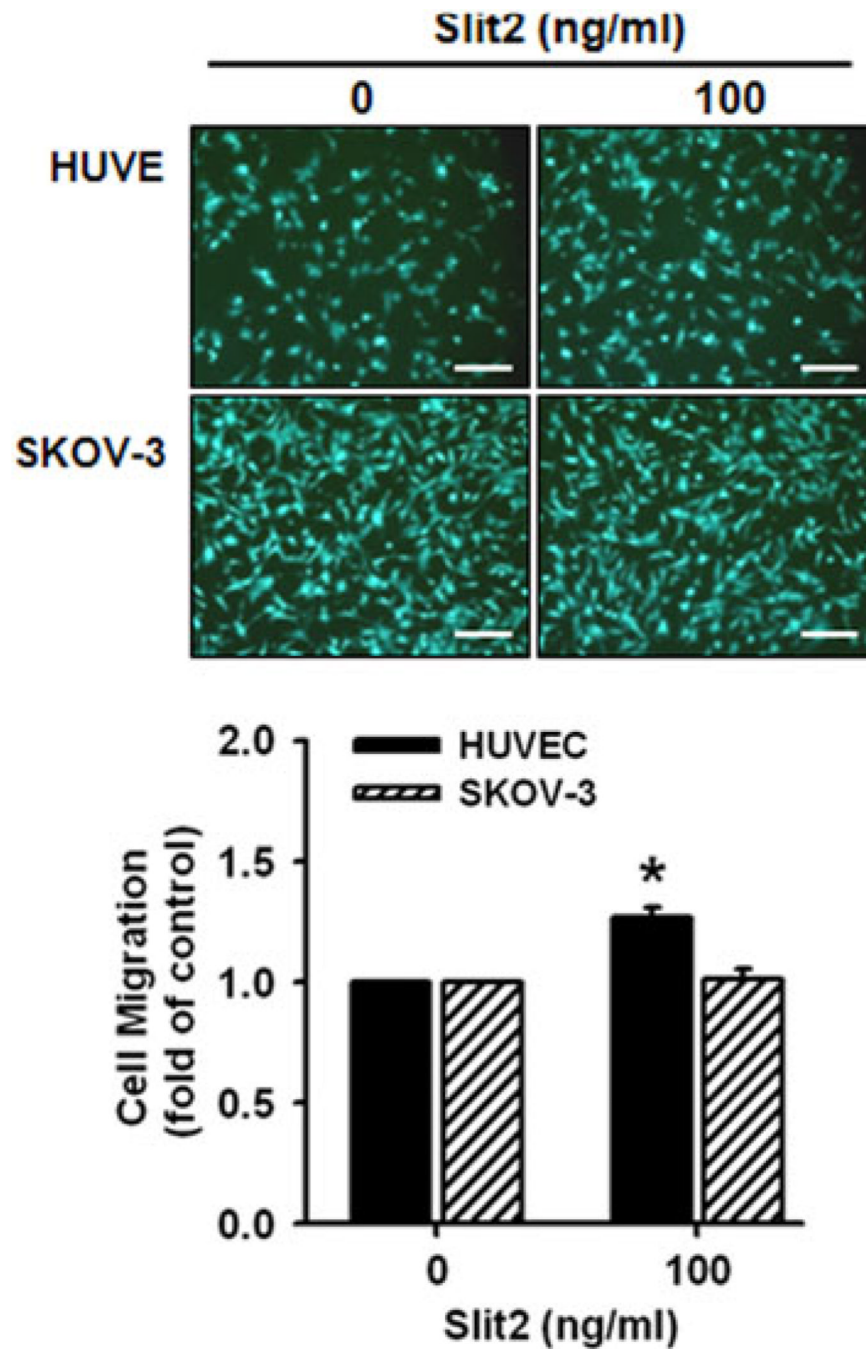


Fig. 4.

Effects of Slit2 on SKOV-3 and HUVE cell migration. After serum starvation, cells were seeded in the inserts. Slit2 (100 ng/ml) in 0.5% FBS (for SKOV-3 cells) or in 1% FBS (for HUVE cells) were added into the bottom wells. After 16 h of treatment, the numbers of migrated cells were counted. Cell migration is expressed as means \pm SEM fold of the control from four independent experiments. The numbers of migrated cells in the control after 16 h of treatment were 990 ± 66.5 and 376 ± 98.5 for SKOV-3 and HUVE cells, respectively.

*Differs from the day 0 control ($p \leq 0.01$). Bars 200 μ m

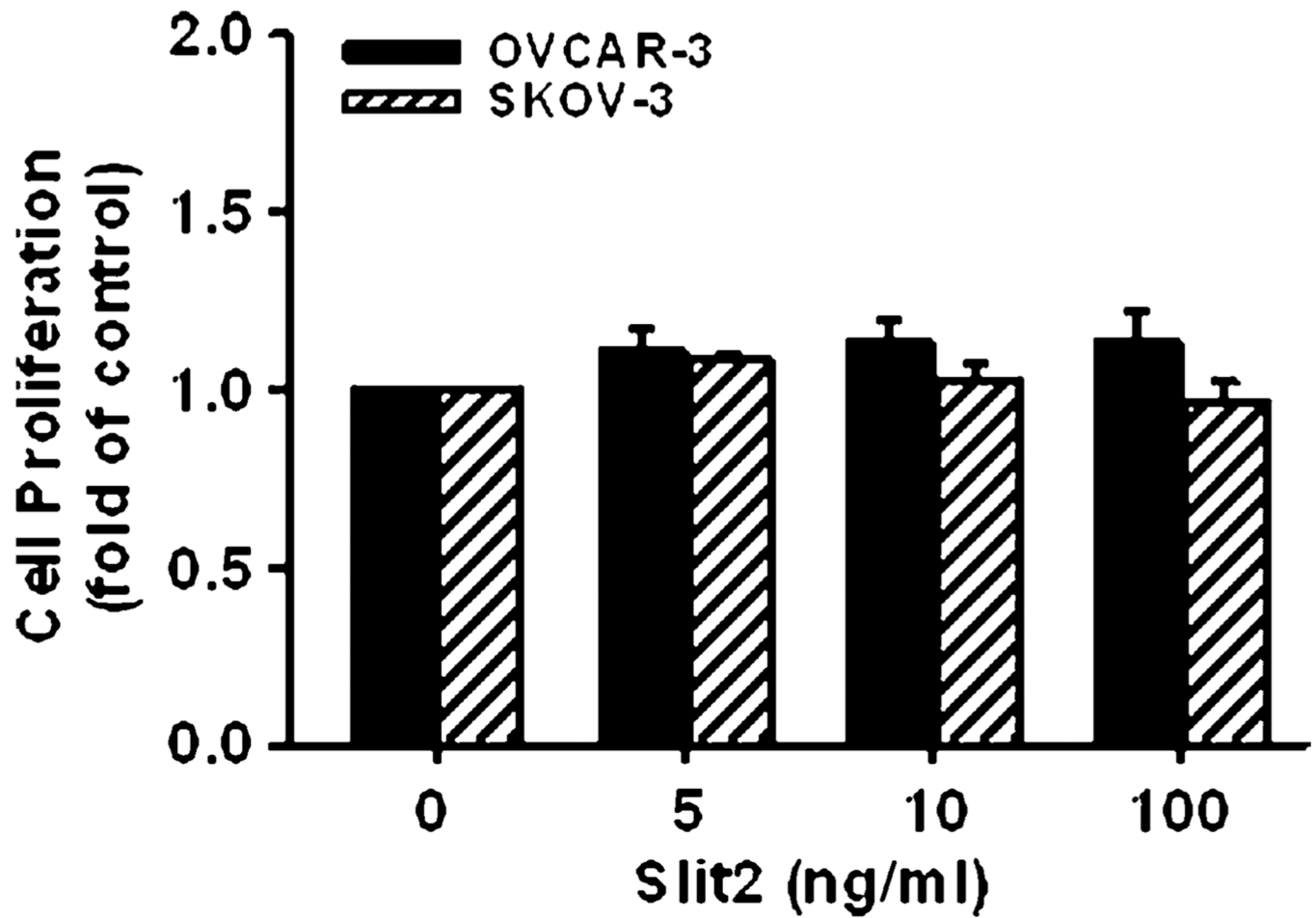


Fig. 5. Effects of Slit2 on OVCAR-3 and SKOV-3 cell proliferation. After serum starvation, cells were treated without or with different doses of Slit2 for 4 days. The media were replaced with fresh Slit2 every 48 h. Cell numbers are expressed as means \pm SEM from three independent experiments

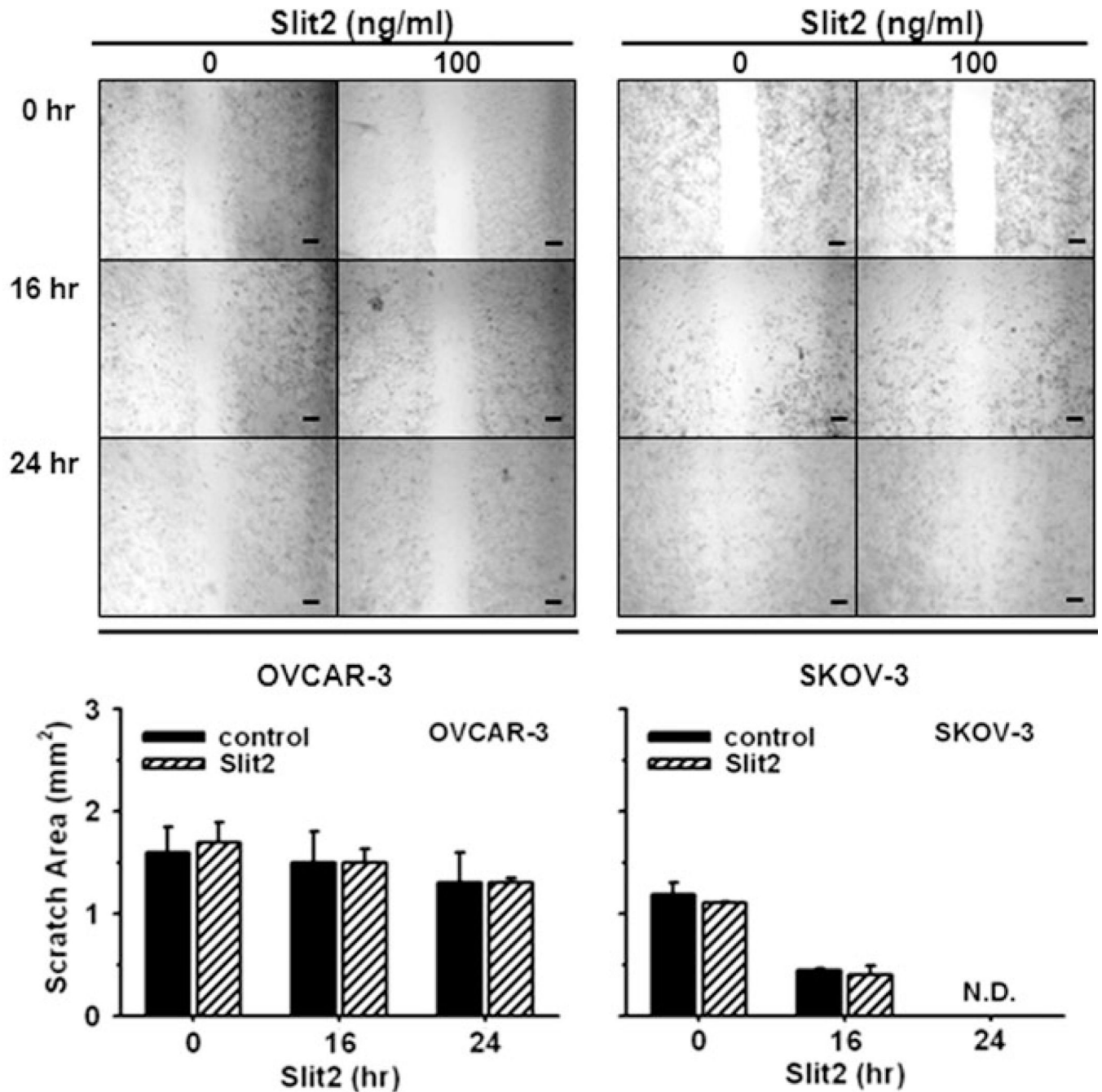


Fig. 6. Effects of Slit2 on the scratch wound healing in OVCAR-3 and SKOV-3 cells. After serum starvation, confluent cells grown on the 12-well plates were scratched followed by treating cells with Slit2 (100 ng/ml) up to 24 h. The scratch areas (mm²) were determined at time 0, 16, and 24 h. Data are expressed as means \pm SEM scratch areas per image from three independent experiments. *ND* not detectable, *Bars* 200 μ m

Table 1

Basal levels of tERK1/2, pERK1/2, tAKT1, and pAKT1 in OVCAR-3 and SKOV-3 cells

	OVCAR-3	SKOV-3
tERK1/2	0.71 ± 0.14	1.62 ± 0.21 [§]
pERK1/2	0.78 ± 0.44	0.92 ± 0.17
tAKT1	1.27 ± 0.50	1.11 ± 0.26
pAKT1	0.26 ± 0.01	1.00 ± 0.22 [§]

Data on total ERK1/2 (tERK1/2) and total AKT1 (tAKT1) were normalized to GAPDH. Data on phospho ERK1/2 (pERK1/2) and phospho AKT1 (pAKT1) were normalized to tERK1/2 and tAKT1, respectively. Data are expressed as means ± SEM

[§]Differs from OVCAR-3 ($p \leq 0.05$, $n = 4$)